Fidelity for the quantum evolution of a Bose-Einstein condensate

Jie Liu,[1,2] Wenge Wang,[1,3] Chuanwei Zhang,[4,5] Qian Niu,[4] and Baowen Li[1,6]
[1]*Department of Physics and the Beijing–Hong Kong–Singapore Joint Center for Nonlinear and Complex Systems (Singapore), National University of Singapore, 117542, Republic of Singapore*
[2]*Institute of Applied Physics and Computational Mathematics, P.O. Box 100088, Beijing, People's Republic of China*
[3]*Department of Physics, Southeast University, Nanjing 210096, People's Republic of China*
[4]*Department of Physics, The University of Texas, Austin, Texas 78712-1081, USA*
[5]*Center for Nonlinear Dynamics, The University of Texas, Austin, Texas 78712-1081, USA*
[6]*Graduate School for Integrative Sciences and Engineering, National University of Singapore, 117597, Republic of Singapore*
(Received 7 September 2005; published 29 December 2005)

We investigate fidelity for the quantum evolution of a Bose-Einstein condensate (BEC) and reveal its general property with a simple two-component BEC model. We find that, when the initial state is a coherent state, the fidelity decays with time in the ways of exponential, Gaussian, and power law, depending on the initial location, the perturbation strength, as well as the underlying mean-field classical dynamics. In this case we find a clear correspondence between the fast quantum fidelity decay and the dynamical instability of the mean-field system. With the initial state prepared as a maximally entangled state, we find that the behavior of fidelity has no classical correspondence and observe an interesting behavior of the fidelity: periodic revival, where the period is inversely proportional to the number of bosons and the perturbation strength. An experimental observation of the fidelity decay is suggested.

DOI: 10.1103/PhysRevA.72.063623 PACS number(s): 03.75.Kk, 05.45.−a, 42.50.Vk

I. INTRODUCTION

The investigation of coherent manipulation of the quantum state of matter and light has provided insights in to many quantum phenomena, in particular, in quantum information processes [1]. The realization of Bose-Einstein condensation (BEC) in dilute gases has provided a different tool for such investigations [2]. In the other aspect, the instability issue of Bose-Einstein condensation (BEC) has been constantly addressed for its crucial role in the control, manipulation, and even future application of this newly formed matter. Dynamical instability [3], Landau or superfluid instability [4], modulation instability [5], and quantum fluctuation instability [6] have been discussed thoroughly. It is found that instability may break the coherence among the atoms and lead to collapse of BEC [7].

However, an important issue is still missing, namely, the sensitivity of the quantum evolution of a BEC with respect to a perturbation from the controlling parameters, or from the outer environment. This instability is distinguished from the instability mentioned above in that the perturbation here is from the outer environment rather than from the inner of the system. It can be depicted by the so-called fidelity, or the Loschmidt echo function, defined as the overlap of two states obtained by evolving the same initial state under two slightly different (perturbed and unperturbed) Hamiltonians [8,9]. This issue is very essential for coherent manipulation of BEC as well as for future application of BEC to quantum information and quantum computation [10,11].

In this paper, we discuss this issue by considering a two-component BEC trapped in a harmonic potential [12], subject to a periodic coupling (successive kicks) between the two components. This is a rather general model containing rich dynamical behavior as we show later; with a constant coupling it is the BEC system proposed recently to generate the entangled state for quantum conputation [11]. Taking this simple model, for example, we investigate the new instability of BEC and reveal its general property. We find that, when the initial state is a coherent state, the fidelity decays with time in the ways of exponential, Gaussian, and power law, depending on the initial location, the perturbation strength, as well as the underlying mean-field classical dynamics. In this case we find clear evidence for the correspondence between the fast quantum fidelity decay and the dynamical instability of the corresponding mean-field system. This fact reveals the quantum essence of the dynamical instability in the mean-field treatment of BEC. With the initial state prepared as a maximally entangled state, we find the behavior of fidelity decay has no classical correspondence and observe an interesting behavior of the fidelity: periodic revival, where the period is inversely proportional to the number of bosons and the perturbation strength. We finally suggest an experimental scheme to observe the fidelity decay with BEC and show that the fidelity instability (fast decay) may lead to a fadeaway of the inference pattern of recent experiments [13].

The paper is organized as follows. In Sec. II we give the physical model. In Sec. III we give the analytic solution to the classical system and plot its phase space. In Sec. IV we discuss the fidelity for the quantum evolution of the coherent states. In Sec. V we discuss the fidelity for the quantum evolution of the entangled states. In Sec. VI we give our conclusions and suggest an experimental scheme for observing the fidelity decay.

II. PHYSICAL MODEL

We consider that cooled ^{87}Rb atoms in a magnetic trap are driven by a microwave coupling into a linear superposition

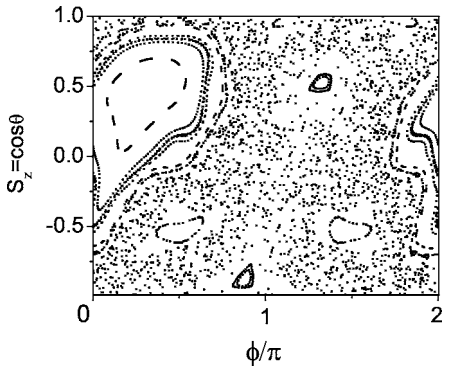

FIG. 1. Periodic snapshot of the orbits for $\mu=T=g_c=1$, $K=2$, where the x axis ϕ is the azimuthal angle. It shows one big island and four small islands. Inside the islands motions are stable, outside the islands motions are mainly unstable or chaotic.

of two different hyperfine states, $F=1$, $m_F=-1$ and $F=2$, $m_F=+1$. A near resonant pulsed radiation laser field is used to couple the two internal states. It is useful in this case to consider the Hamiltonian in a rotating frame, where the laser field is constant over a time of pulse. The total density and mean phase remain constant during the condensate evolution. Within the standard rotating-wave approximation, the Hamiltonian describing the transition between the two internal states reads

$$\hat{H}=\frac{\mu}{2}(\hat{a}_1^\dagger\hat{a}_1-\hat{a}_2^\dagger\hat{a}_2)+\frac{g}{4}(\hat{a}_1^\dagger\hat{a}_1-\hat{a}_2^\dagger\hat{a}_2)^2+\frac{K}{2}\delta_T(t)(\hat{a}_1^\dagger\hat{a}_2+\hat{a}_2^\dagger\hat{a}_1), \tag{1}$$

where $\delta_T(t)$ represents $\Sigma_n\delta(t-nT)$, K is the coupling strength proportional to the laser field. Here we suppose that the laser field used to couple the two states is only turned on at certain times of a period T. $\hat{a}_1,\hat{a}_1^\dagger,\hat{a}_2$, and $\hat{a}_2^\dagger$ are boson annihilation and creation operators for the two components, respectively. $K=\hbar\Omega_R$, $g=(2\pi\hbar^2/m)\eta(2a_{12}-a_{11}-a_{22})$, $\mu=-\delta+(4N\pi\hbar^2/m)\eta(a_{11}-a_{22})$. In the above parameters, Ω_R is the Rabi frequency; a_{ij} is the s-wave scattering amplitude; δ is the detuning of lasers from resonance, very small and negligible in our case; N is the atom number; m is the mass of atom; η is a constant of order 1 independent of the hyperfine index, relating to an integral of equilibrium condensate wave function [14].

Writing the above Hamiltonian in terms of the SU(2) generators [15], $\hat{L}_x=(\hat{a}_1^\dagger\hat{a}_2+\hat{a}_2^\dagger\hat{a}_1)/2$, $\hat{L}_y=(\hat{a}_1^\dagger\hat{a}_2-\hat{a}_2^\dagger\hat{a}_1)/2i$, $\hat{L}_z=(\hat{a}_1^\dagger\hat{a}_1-\hat{a}_2^\dagger\hat{a}_2)/2$, we have $\hat{H}=\mu\hat{L}_z+g\hat{L}_z^2+K\delta_T(t)\hat{L}_x$. The three angular momentum operators satisfy the Heisenberg equation $i(d/dt)\hat{L}_i=[\hat{L}_i,\hat{H}]$ $(i=x,y,z)$, and $[\hat{L}_x,\hat{L}_y]=i\hat{L}_z$ with cyclic permutation. The Planck constant is set to be unit here and in what follows. The Floquet operator describing the quantum evolution in one period is

$$\hat{U}=\exp[-i(\mu\hat{L}_z+g\hat{L}_z^2)T]\exp(-iK\hat{L}_x). \tag{2}$$

The Hilbert space spanned by the eigenstates of $\hat{L}_z$, $|l\rangle$ with $l=-L,-L+1,\ldots,L$, where $L=N/2$. The above system demonstrates rich dynamical behaviors, and will degenerate to the quantum kicked top model for some specific choice of the parameters [16]. As in the kicked top model, an effective Planck constant can be introduced, $\hbar_{\text{eff}}=1/L$, which will be written as $\hbar$ for brevity.

III. CLASSICAL MOTIONS

Before going to the study of the quantum evolution of the above system and demonstrating the decay of the Loschmidt echo function under a slight perturbation on the Hamiltonian, we first study the classical dynamics of the system in the absence of external perturbation. Later we will show its connection to the quantum fidelity instability

The system considered has a classical counterpart in the limit $N\to\infty$, where N is the total number of the atoms, describing a spin moving on a Bloch sphere with $S_i=(1/L)\times\langle\hat{L}_i\rangle$ $(i=x,y,z)$. The classical Hamiltonian takes the form $H=\mu S_z+g_cS_z^2+K\delta_T(t)S_x$, where $g_c=gL$. Their motions are governed by $\dot{S}_i=[S_i,H]_{cl}$ $(i=x,y,z)$, with relation $[S_x,S_y]_{cl}=S_z$ and cyclic permutation. The above equations give the motion of the center of a coherent quantum wave packet ignoring the quantum fluctuation, equivalent to the mean-field Gross-Pitaevskii (GP) equation with a time-dependent potential. Technically, to obtain the mean-field classical model, we need to focus on the Gross-Pitaevskii state $|\Psi_{gp}\rangle=(1/\sqrt{N!})(a_1\hat{a}_1^\dagger+a_2\hat{a}_2^\dagger)^N|\text{vac}\rangle$. By computing the expectation value $\langle\hat{H}\rangle=\langle\Psi_{gp}|\hat{H}|\Psi_{gp}\rangle$, one obtains the mean-field Hamiltonian $H_{mf}=\langle\hat{H}\rangle/N$ in the limit $N\to\infty$. The mean-field Hamiltonian will give the classical dynamics discussed above.

The classical motion for one period can be solved analytically, with the free evolution between two consecutive kicks corresponding to an angle $(\mu+2g_cS_z)T$ rotation around the S_z axis, that is

$$S'_z=S_z, \tag{3}$$

$$S'_x=S_x\cos(\mu+2g_cS_z)T-S_y\sin(\mu+2g_cS_z)T, \tag{4}$$

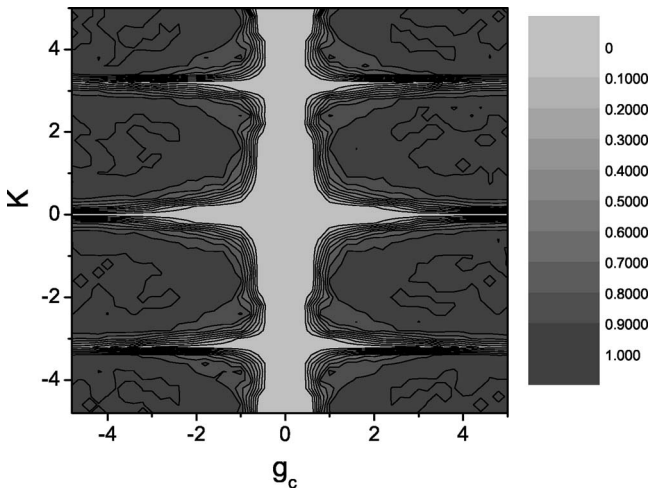

FIG. 2. Contour plot of the fraction of chaotic motions for $\mu=T=1$.

$$S'_y = S_x \sin(\mu + 2g_c S_z)T + S_y \cos(\mu + 2g_c S_z)T. \quad (5)$$

The periodic kick added at discrete time nT corresponds to an angle K rotation around the S_x, that is

$$S'_x = S_x, \quad (6)$$

$$S'_y = S_y \cos(K) - S_z \sin(K), \quad (7)$$

$$S'_z = S_y \sin(K) + S_z \cos(K). \quad (8)$$

If initially we have a small deviation $(\delta S_x, \delta S_y, \delta S_z)$, during one periodic evolution the deviation will be magnified, $(\delta S'_x, \delta S'_y, \delta S'_z)^\dagger = D \circ (\delta S_x, \delta S_y, \delta S_z)^\dagger$, where the tangent map takes the form, with $\alpha = (\mu + 2g_c S_z)T$, $\beta = K$,

$$D(S_x, S_y, S_z) = \begin{pmatrix} \cos\alpha & -\sin\alpha & -2g_c T S_x \sin\alpha - 2g_c T S_y \cos\alpha \\ \sin\alpha\cos\beta & \cos\alpha\cos\beta & -\sin\beta + \cos\beta(2g_c T S_x \cos\alpha - 2g_c T S_y \sin\alpha) \\ \sin\alpha\sin\beta & \cos\alpha\sin\beta & \cos(K) + \sin(K)(2g_c T S_x \cos\alpha - 2g_c T S_y \sin\alpha) \end{pmatrix}.$$

Classically, there are two types of motion, classified by magnification of initial deviation: If the magnification is exponential in time, the motion is unstable and chaotic; otherwise, it is stable. In the stable case, the largest Lyapunov exponent, defined as $\lambda = \lim_{n\to\infty}(1/n)\Sigma_n \ln[\|(\delta S'_x, \delta S'_y, \delta S'_z)\|/\|(\delta S_x, \delta S_y, \delta S_z)\|]$, tends to zero. For the unstable case, the exponent is positive. In Fig. 1, we plot the snapshots of the orbits at times of multiple period and get the Poincaré section of the phase space for a pair of variables (S_z, ϕ), i.e., z-component spin and the azimuthal angle. It shows one big island and four small islands. Inside the islands motions are stable, outside the islands motions are mainly unstable or chaotic. The phase structure changes with the parameters. To give an outline picture, we make a large numerical exploration on the parameters (K, g_c). For each pair of parameters, we choose a few thousand initial points randomly on the phase space and then trace their orbits and judge their stability by Lyapunov exponents, then we make statistics on the fraction of the unstable orbits. The results are plotted in Fig. 2. As seen, the integrable cases (all orbits are stable with zero Lyapunov exponents) are the vertical line $g_c = 0$ and horizontal lines $K = n\pi$ with integer n, implying that both nonlinearity and the kick are essential in inducing chaos. When K is an odd multiple of π, the situation is interesting where all orbits bounce between two points separately, corresponding to a phenomenon called the antiresonance case as discussed in our recent paper [7]. Near these strict integrable regimes, the system shows the near-integrable property that almost all orbits are stable except for tiny chaotic layers. In the dark regime of Fig. 2 the system may show strong nonintegrability that the phase space is full of chaotic orbits. In the transition from the integrable regime to the fully chaotic regime, the phase space is the mix of regular orbits and chaotic orbits as shown in Fig. 1. We call it the regime of the mixed case.

IV. FIDELITY FOR QUANTUM COHERENT STATES

The outer perturbation is mimicked by a small change on the interaction parameter or in the coupling strength, etc. Without losing generality, here we suppose that perturbation is applied on the coupling, i.e., a small perturbation leads to the change of the coupling strength like $K \to K + \varepsilon$. With denoting the unperturbed Hamiltonian by H, the perturbed Hamiltonian is written as $H_\epsilon = H + \epsilon V$. The corresponding evolution operator is denoted by $\hat{U}_\epsilon$.

To investigate the influence of the perturbation on the quantum evolution, we need to trace the temporal evolution of the fidelity $M(t) = |m(t)|^2$, where $m(t)$ is the Loschmidt echo defined as

$$m(t = nT) = \langle \Phi_0 | (\hat{U}_\epsilon^\dagger)^n \circ (\hat{U})^n | \Phi_0 \rangle, \quad (9)$$

with $|\Phi_0\rangle$ as the initial state. Fast decay of the fidelity means rapid loss of the information during quantum evolution in presence of outer perturbation. In this section we set the initial state of the BEC $|\Phi_0\rangle$ as a coherent state, centered at sphere with polar angle θ and azimuthal angle ϕ,

$$|\Phi_0\rangle = |\theta, \phi\rangle \equiv e^{\kappa^* L_+ - \kappa L_-} |-L\rangle, \text{ with } \kappa = \frac{\pi - \theta}{2} e^{-i\phi}. \quad (10)$$

We discuss fidelity decay in three typical situations, in which the corresponding mean-field classical system is fully chaotic, near-integrable, and mixed, respectively.

For the parameters $K = 2$, $g_c = 4$, the phase space is fully chaotic. Because of the ergodicity of the chaotic orbits, fidelity decay is expected to be independent on the initial condition. However, it strongly depends on the perturbation strength. As we see in Fig. 3, for a small perturbation, fidelity shows a slow Gaussian decay,

$$M(t) \simeq \exp\left(-\frac{g_n K(E)}{\pi d}\sigma^2 t^2\right), \quad (11)$$

where $\sigma = \epsilon/\hbar$, $g_n = 2$ is the number of classical orbits with identical action, $d = (2L+1)/2\pi$ is the mean density of states, and $K(E)$ is the classical action diffusion constant, $K(E) = \int_0^\infty dt \langle V[r(t)] V[r(0)] \rangle$ with $V[r(t)]$ evaluated along a trajectory.

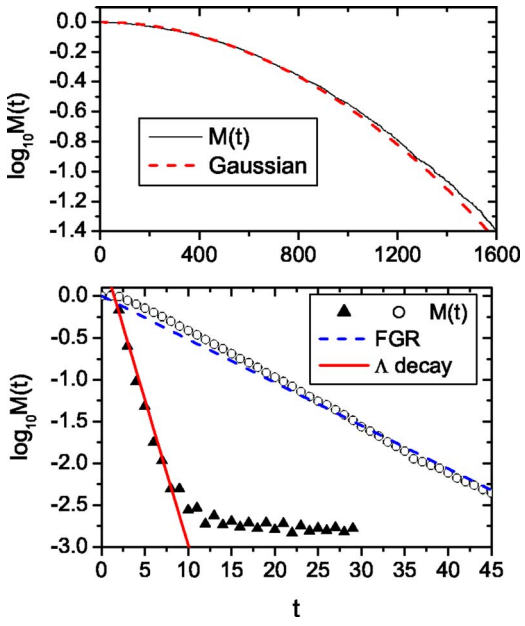

FIG. 3. (Color online) Fidelity decay in a classically chaotic case, with $K=2$, $g_c=4$, $\mu=1$, $T=1$. Upper panel: An example in the perturbative regime with $S=100$, $\epsilon=2\times10^{-4}$, obtained from one initial coherent state. The dashed curve is the theoretical prediction in Eq. (11). Lower panel: Two examples in the FGR and Lyapunov regimes, respectively. In the FGR regime, $S=200$, $\epsilon=3\times10^{-3}$, and an average is performed over 20 initial coherent states taken randomly. The dashed line is the FGR decay. In Lyapunov regime, $S=500$, $\epsilon=1\times10^{-2}$, with an average over 1000 initial coherent states. The solid line is $e^{-\gamma t}$ with $\gamma=\Lambda$ $(t=6)$ in Eq. (14).

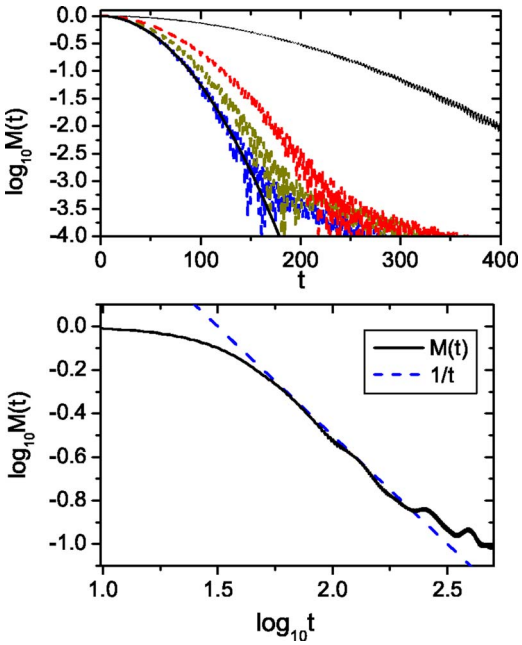

FIG. 4. (Color online) Fidelity decay in a classically nearly integrable case, with $K=2$, $g_c=0.2$, $\mu=1$, $T=1$, $N=200$, and $\epsilon=0.003$. Upper panel: Fidelity of four randomly chosen initial coherent states, with the smooth solid curve being the Gaussian fit to one of them. Lower panel: Averaged fidelity, with an average performed over 50 initial coherent states chosen randomly.

With increasing perturbation strength, one meets a perturbation border ϵ_p at which the typical transition matrix element of perturbation between quasienergy eigenstates becomes larger than the average level spacing [17],

$$\epsilon_p \sim \hbar \sqrt{\frac{\ln(2L+1)}{2K(E)(2L+1)}} \propto \hbar/\sqrt{2L+1}. \tag{12}$$

Above the border the fidelity shows the exponential decay [17,18]; for this case one should distinguish between two regimes, namely, (i) the Fermi-golden-rule (FGR) regime for relatively small ϵ, with an exponential decay

$$M(t) \propto e^{-\Gamma t}, \tag{13}$$

where $\Gamma=2\sigma^2K(E)$ [17]; and (ii) the Lyapunov regime for relatively large ϵ, in which the fidelity decay as $e^{-\lambda t}$ for systems whose underlying classical dynamics has a constant local Lyapunov exponent λ [19]. When the classical system has non-negligible fluctuation in the finite-time Lyapunov exponent, the fidelity has the following decay at large enough ϵ [20,21]:

$$\bar{M}(t) \propto e^{-\Lambda(t)t}, \text{ with } \Lambda(t) = -\frac{1}{t}\ln\left|\frac{\delta x(t)}{\delta x(0)}\right|^{-1}, \tag{14}$$

where $\delta x(t)$ indicates distance in phase space and the average is performed over phase space. Figure 3 shows typical fidelity decay for the three cases and detailed parameters are indicated in the caption.

As we choose parameters as $K=2$, $g_c=0.2$, the classical system is nearly integrable where the phase space is full of periodic and quasiperiodic orbits. We found Gaussian decay for the fidelity of single initial coherent states, with a strong dependence of decaying rate on the location of the initial coherent states. The Gaussian decay may be followed by a power-law decay $1/t^{\eta}$ with $\eta \geqslant 1$ for the large time scale. However, after averaging over the whole phase space, we find that the fidelity decay can be well fitted by an inverse power law $1/t$, as shown in Fig. 4. In this case, for the quantum evolution of initial coherent state BEC, high fidelity can be expected, because the fidelity has a slow power-law decay on average.

Now we turn to the mixed case, which is more complicated than the previous two cases. It is usually expected that fidelity decay of initial coherent states lying in regular regions would be similar to that in a nearly integrable system, and that from chaotic regions they would be similar to that in a chaotic system. However, we find that this naive picture is not exact. Let us take the mixed system with the parameters the same as in Fig. 1 for an example and first discuss initial coherent states lying within the regular regions. We find that fidelity of such states has quite a slow decay, contrary to what is shown in the upper panel of Fig. 4. In particular, for initial coherent states lying in the largest regular region, fidelity remains close to 1, even at $t=200$, as shown in Fig. 5. Note that the quantum perturbation strength characterized by $\sigma=\epsilon/\hbar$ has the same value in Figs. 4 and 5. This phenomenon cannot be explained by means of expanding the coher-

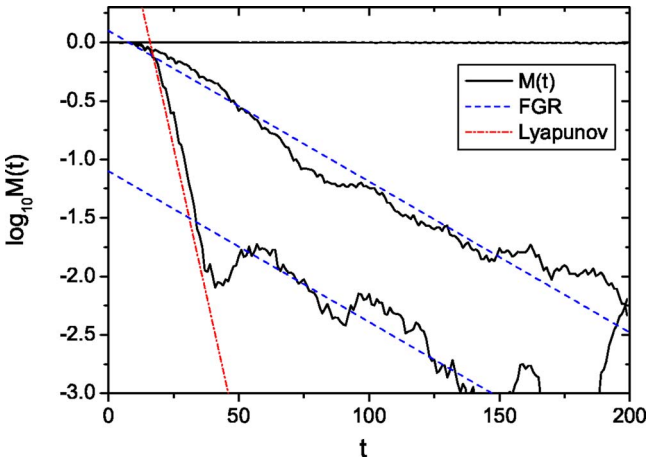

FIG. 5. (Color online) Fidelity decay in the mixed system whose classical phase space structure is shown in Fig. 1. $L=500$ and $\epsilon=0.0006$, so that $\sigma=\epsilon/\hbar=0.3$. The almost nondecaying solid line is the fidelity of an initial coherent state lying within the largest regular region. The other two solid curves, one close to the FGR decay, the other first having a Lyapunov decay then an approximately FGR decay, correspond to the fidelity of two initial coherent states lying in the chaotic region of the classical system.

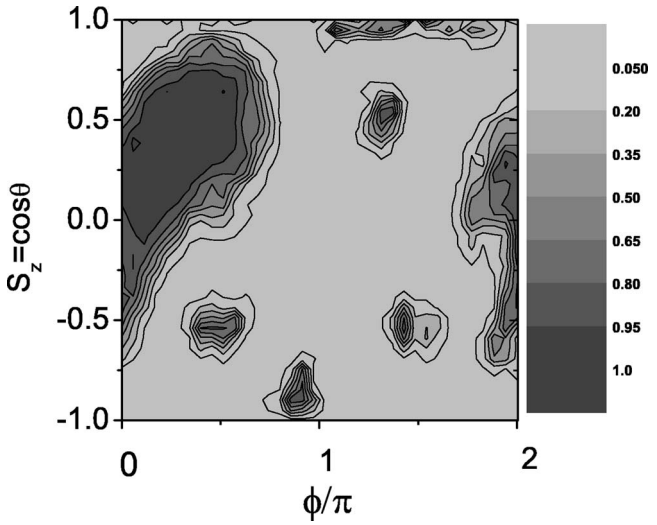

FIG. 6. Contour plot of the fidelity $M(t)$ at $t=200$, for $K=2$, $g_c=\mu=T=1$, $N=1000$, and $\epsilon=0.0006$, with the classical phase space possessing a mixed structure shown in Fig. 1.

ent states in the eigenstates of the systems, as done in Ref. [8] for angular momentum eigenstates in the system there, since the values of the participation function of the coherent states, defined by $1/(\Sigma_\alpha|\langle\alpha|\Phi_0\rangle|)^4$, are not small. Indeed, for example, for the state giving the almost nondecaying fidelity in Fig. 5, the participation function is larger than 22. We mention that this phenomenon implies that quantum motion in the regular region of a mixed system can be more stable than that in a corresponding unperturbed (integrable) system.

In the above mixed system, fidelity of initial coherent states coming from chaotic regions also exhibit unexpected behaviors. For a chaotic system, $\sigma=0.3$ belongs to the FGR regime and the fidelity has the FGR decay Eq. (13) as shown in Fig. 3. However, in the mixed system with $\sigma=0.3$, the fidelity of initial coherent states lying within the chaotic region has not only FGR decay, but also faster decays, even as fast as the Lyapunov decay at the beginning time (see Fig. 5). It was found that typical decay of fidelity in this system is either close to the FGR decay or between the Λ decay and the Lyapunov decay.

In order to have a knowledge of the global situation of fidelity decay in a mixed system, we show a contour plot for $M(t=200)$ in Fig. 6. This picture illustrates similar structure of Fig. 1. The similarity can be understood from different dispersion behaviors of the coherent-state wave packets starting from regular regions and chaotic regions, respectively. Compared to that in the regular region, in the chaotic region the wave packets disperse much faster and soon become extended (for example) in the ϕ representation. We then imagine that the overlap of two states governed by slightly different (perturbed and unperturbed) Hamiltonians may decay fast with time. It means that the dynamical instability regime of the classical system usually corresponds to the low fidelity regime of the quantum system. On the other hand, inside the islands (large or small) where the classical motions are dynamically stable with zero Lyapunov exponent, the fidelity shows different behavior: The fidelity in the large island is higher than that in the small islands. In the connected chaotic region where the Lyapunov exponent has a certain positive value, the fidelity may show different behaviors as shown in Fig. 5. These facts on the other hand elucidate that fidelity contains more information about the system under a perturbation and therefore is a more general quantity to describe the stability of the BEC.

V. FIDELITY FOR ENTANGLED STATES

In the above discussions we set the initial states as coherent states. Actually, the quantum degenerate atomic gases is a fertile ground for exploring applications in quantum information, where the entangled state plays a crucial role. Discussing fidelity of the entangled state is of great interest and of practical significance. Therefore in the following discussions we assume a maximum entangled state or N-GHZ (Greenberger-Horne-Zeilinger) state is generated initially [11], which can be written as follows for our N-bosons system:

$$|\mathrm{GHZ}\rangle_N=\frac{1}{\sqrt{2}}\left(\frac{\hat{a}_1^{\dagger N}}{\sqrt{N!}}+\frac{\hat{a}_2^{\dagger N}}{\sqrt{N!}}\right)|0\rangle=\frac{1}{\sqrt{2}}(|-L\rangle+|L\rangle). \quad (15)$$

We want to discuss the fidelity for its quantum evolution.

Before presenting our numerical results, we make some simple deductions and give a theoretical prediction for the fidelity behavior of the entangled state. Supposing the perturbation is very small, we can ignore the term like $\langle L|(\hat{U}_\epsilon^\dagger)^n\circ(\hat{U})^n|-L\rangle$ (this assumption is more suitable for the near-integrable case, where the evolution of the quantum states is expected to be localized due to invariant tori). Then the Loschmidt echo function for the GHZ state may simply be expressed as the sum of the echo functions of the Fock states $|-L\rangle$ and $|L\rangle$, namely,

$$m_{|GHZ\rangle}(t) \simeq \frac{1}{2} m_{|L\rangle}(t) + \frac{1}{2} m_{|-L\rangle}(t). \tag{16}$$

If the difference between the echo functions of the two Fock states $[\|m_{|L\rangle}(t)| - |m_{|-L\rangle}(t)\|]$ is large, the interference terms in the fidelity expression of the GHZ state will be negligible, the fidelity of the GHZ state will be approximate to the fidelity of one Fock state that has large absolute echo function, showing a monotonous decrease with time. On the other hand, if the echo functions of the two Fock states are comparable, the fidelity of the GHZ state will show an oscillation between minimum $\frac{1}{4}\|m_{|L\rangle}(t)| - |m_{|-L\rangle}(t)\|^2$ and maximum $\frac{1}{4}\|m_{|L\rangle}(t)| + |m_{|-L\rangle}(t)\|^2$. The period of this oscillation, denoted by T_{ent}, is determined by the relative phase between the echo functions of the two Fock states.

In the nearly integrable case, the dependence of T_{ent} on the effective Planck constant $\hbar$ as well as on ϵ can be estimated as follows. In a uniform semiclassical approach, it has been found that the phase of the fidelity of a coherent state is roughly given by the quantity

$$\Delta S \simeq \frac{\epsilon}{\hbar} \int_0^t dt' V[r(t')] \tag{17}$$

with the value of $V[r(t')]$ evaluated along the classical trajectory starting at the center of the initial coherent state [19]. Here ϵV is the perturbation, ΔS is in fact the action difference along two nearby trajectories starting at the same point in the phase space of the two systems H and H_0. In nearly an integrable system, due to the quasiperiodicity of trajectories, the integral on the right-hand side of Eq. (17) is approximately proportional to t at long time. Then, the phase difference for the fidelity of two initial coherent states centered at different regions of the phase space, is proportional to $\epsilon L t$. Note that the Wigner functions of the two Fock states $|L\rangle$ and $|-L\rangle$ occupy distant regions in phase space. Expanding the two Fock states in coherent states, we find that the relative phase of $m_{|L\rangle}(t)$ and $m_{|-L\rangle}(t)$ is approximately proportional to $\epsilon L t$ as well, implying that $T_{\text{ent}} \propto 1/(\epsilon L)$.

Our numerical simulations prove the above theoretical predictions, as shown in Fig. 7. The periodic oscillation in the upper panel of Fig. 7 is quite aninteresting phenomenon; it indicates that the fidelity already decayed very low can revive after a certain time duration. This type of fidelity behavior is a unique property for the entangled state.

In the lower panel of Fig. 7, we set a larger nonlinearity parameter, $g_c=1$, which falls into the mixed regime with the phase space demonstrated in Fig. 1. We plot the temporal evolution of fidelity for the two Fock states $|-L\rangle$ and $|L\rangle$, as well as for the GHZ state. We find that the behavior of the fidelity of the GHZ state can be well fitted by a Gaussian decay. Comparing this result with the coherent state case in Fig. 5, we find a big difference. It reflects the pure quantum property of the GHZ state.

To have a knowledge of the global situation of fidelity decay for the GHZ states with respect to the system's parameters, we calculate the fidelity for a wide range of parameters

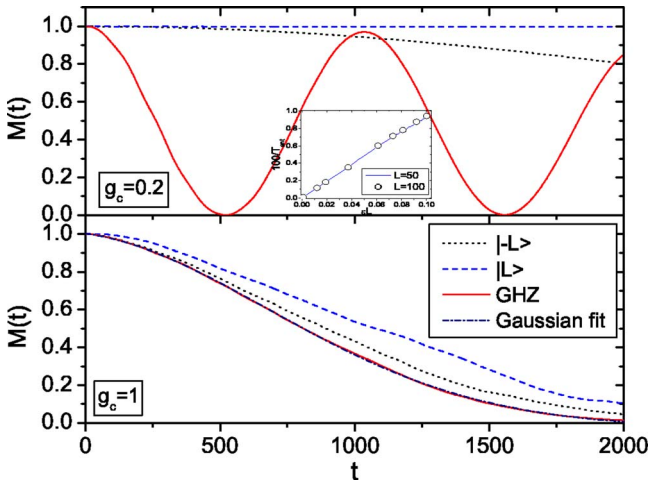

FIG. 7. (Color online) Fidelity for the two Fock states and the GHZ entangled state, with $L=500$, $\epsilon=2\times10^{-5}$, and $K=2$. The upper panel is with $g_c=0.2$. Inset of upper panel: $100/T_{\text{ent}}$ vs ϵL for ϵL from 0.001 to 0.1, with $L=50$ (solid line) and $L=100$ (circles), showing the linear dependence of T_{ent} on $1/\epsilon L$. The lower panel is for $g_c=1$, in which the fidelity of the GHZ state can be well fitted by a Gaussian decay.

as shown in Fig. 8. Comparing with the contour plot of classical dynamics in Fig. 2, we find no clear evidence for the correspondence.

VI. CONCLUSIONS AND EXPERIMENTAL SUGGESTIONS

In conclusion, we have investigated the instability of a BEC under an external perturbation. When the initial state is a coherent state, the fidelity decay has a close relation to the mean-field classical dynamics. This correspondence reveals the quantum essence of the dynamical instability of the classical mean-field equation (GP equation) of BECs. As well known, a BEC system is essentially a quantum many-body

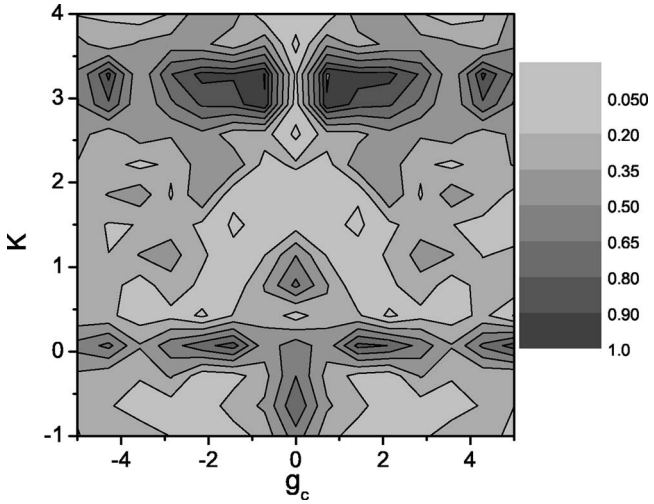

FIG. 8. Contour plot of the fidelity $M(t)$ at $t=1500$, with respect to the parameters g_c, K. The initial quantum states are the GHZ entangled state.

problem, governed by linear Schrodinger equation. It should not be sensitive to small change in its initial condition. However, as the zeroth-order approximation (1/N), the mean-field GP equation surely has the dynamical instability characterized by the sensitivity on a small initial condition. This leaves a puzzle about the quantum source of the dynamical instability. Our discussions provide an explanation to this puzzle, that the dynamical instability of the GP equation is the classical manifestation of the fidelity instability of the original quantum system. This argument is strongly supported by our numerical calculations. We also discuss the fidelity for the maximally entangled state and find a purely quantum behavior without classical correspondence. We observe an interesting behavior of the fidelity: periodic revival, where the period is inversely proportional to the number of bosons and the perturbation strength. Our theoretical analysis provide a good explanation for the above phenomenon.

This instability characterized by the fast fidelity decay may lead to an observable phenomenon. Here we propose an experiment to observe the fidelity decay. Let us consider BECs (e.g., ^{87}Rb) that are optically cooled and trapped and are then transferred into a double-well potential. The double-well potential can be created by focusing blue-detuned far-off-resonant laser light into the center of the magnetic trap [22], or by deforming single-well optical trap into a double-well potential with linearly increasing the frequency difference between the rf signals [13]. In both systems the interference between the two condensates is observed by simultaneously switching off the magnetic or optical trap and the laser-light sheet. To observe the fidelity instability due to the internal dynamics, before switching off the traps, we apply near-resonant coupling fields to the condensates to couple the two hyperfine states of ^{87}Rb, e.g., $F=1$, $m_F=-1$ and $F=2$, $m_F=+1$ like in Ref. [12], with a slightly different strength in the two wells. The condensate in each well can then dynamically convert between internal states. Then switching off the traps and letting the two clouds of BEC expand, our prediction of the fast decay of the system's fidelity will lead to fadeaway of the inference pattern. This can be understood from the formula $I \propto |\psi_1\chi_1|^2 + |\psi_2\chi_2|^2 + 2\mathrm{Re}(\psi_1^*\psi_2\chi_1^*\chi_2)$ with 1, 2 labeling the wells. Clearly, high fidelity of the two internal states χ corresponds to high visibility of the interference. Here we require that the wells be deep, so that the total density remains relatively constant. The atom number in each well is nearly equal. Small fluctuations on the atom number does not essentially affect our predictions since it may be regarded as another perturbation source.

ACKNOWLEDGMENTS

The work was supported in part by a Faculty Research Grant of National University of Singapore, DSTA Singapore under Project Agreement No. POD0410553 (B.L.), the NSF of China Grant No. 10275011 (W.W.), and the NSF of the US. J.L. is supported by the NSF of China (10474008), the NFRP of China (2005CB3724503), and the 863 project (2004AA1Z1220).

[1] M. D. Lukin, Rev. Mod. Phys. **75**, 457 (2003).
[2] M. H. Anderson *et al.*, Science **269**, 198 (1995);K. Davis *et al.*, Phys. Rev. Lett. **75**, 3969 (1995);C. C. Bradley *et al.*, *ibid.* **75**, 1687 (1995).
[3] S. Sinha and Y. Castin, Phys. Rev. Lett. **87**, 190402 (2001);P. Buonsante, R. Franzosi, and V. Penna, Phys. Rev. Lett. **90**, 050404 (2003).
[4] L. J. Garay, J. R. Anglin, J. I. Cirac, and P. Zoller, Phys. Rev. Lett. **85**, 4643 (2000).
[5] V. V. Konotop and M. Salerno, Phys. Rev. A **65**, 021602(R) (2002);L. Salasnich, A. Parola, and L. Reatto, Phys. Rev. Lett. **91**, 080405 (2003);L. D. Carr and J. Brand, *ibid.* **92**, 040401 (2004).
[6] J. R. Anglin and A. Vardi, Phys. Rev. A **64**, 013605 (2001);V. A. Yurovsky, *ibid.* **65**, 033605 (2002);G. P. Berman, A. Smerzi, and A. R. Bishop, Phys. Rev. Lett. **88**, 120402 (2002).
[7] Jie Liu, Biao Wu, and Qian Niu Phys. Rev. Lett. **90**, 170404 (2003);C. Zhang, J. Liu, M. G. Raizen, and Q. Niu, *ibid.* **92**, 054101 (2004); **93**, 074101 (2004).
[8] A. Peres, Phys. Rev. A **30**, 1610 (1984).
[9] W. Wang and B. Li, Phys. Rev. E **66**, 056208 (2002);W. Wang, G. Casati, and B. Li, *ibid.* **69**, 025201(R) (2004);W. Wang and B. Li, *ibid.* **71**, 066203 (2005), and references therein.
[10] M. A. Nielsen and I. L. Chuang, *Quantum Computation and Quantum Information* (Cambridge University Press, Cambridge, England, 2000).
[11] L. You, Phys. Rev. Lett. **90**, 030402 (2003);M. Zhang and L. You, *ibid.* **91**, 230404 (2003);A. P. Hines, R. H. McKenzie, and G. J. Milburn, Phys. Rev. A **67**, 013609 (2003).
[12] M. R. Matthews, B. P. Anderson, P. C. Haljan, D. S. Hall, M. J. Holland, J. E. Williams, C. E. Wieman, and E. A. Cornell, Phys. Rev. Lett. **83**, 3358 (1999).
[13] Y. Shin, M. Saba, T. A. Pasquini, W. Ketterle, D. E. Pritchard, and A. E. Leanhardt, Phys. Rev. Lett. **92**, 050405 (2004).
[14] A. J. Leggett, Rev. Mod. Phys. **73**, 307 (2001).
[15] A. Vardi and J. R. Anglin, Phys. Rev. Lett. **86**, 568 (2001).
[16] F. Haake, *Quantum Signature of Chaos* (Springer-Verlag, New York, 2000).
[17] N. R. Cerruti and S. Tomsovic, Phys. Rev. Lett. **88**, 054103 (2002); J. Phys. A **36**, 3451 (2003).
[18] Ph. Jacquod, P. G. Silvestrov, and C. W. J. Beenakker, Phys. Rev. E **64**, 055203(R) (2001).
[19] R. A. Jalabert and H. M. Pastawski, Phys. Rev. Lett. **86**, 2490 (2001).
[20] P. G. Silvestrov, J. Tworzydło, and C. W. J. Beenakker, Phys. Rev. E **67**, 025204(R) (2003).
[21] Wen-ge Wang, G. Casati, B. Li, and T. Prosen, Phys. Rev. E **71**, 037202 (2005).
[22] M. R. Andrews *et al.*, Science **275**, 637 (1997).